THE ASTROPHYSICAL JOURNAL, 293:294–302, 1985 June 1

AN ANALYSIS OF THE BRIGHT WHITE DWARF CD −38°10980

J. B. HOLBERG[1]
Lunar and Planetary Laboratory, University of Arizona
F. WESEMAEL
Département de Physique and Observatoire du mont Mégantic, Université de Montréal
G. WEGNER
Department of Physics and Astronomy, Dartmouth College
AND
F. C. BRUHWEILER[1]
Department of Physics, Catholic University of America
Received 1984 October 2; accepted 1984 December 10

ABSTRACT

The bright DA white dwarf CD −38°10980 is comprehensively analyzed using all available data. Detailed comparisons of the overall energy distribution and Lyman-α and Balmer profiles are made with theoretical predictions based on a homogeneous grid of model atmospheres. These comparisons yield a consistent, well-defined effective temperature and surface gravity for this star of 24,700 ± 250 K and log $g = 7.95 \pm 0.15$, respectively. A new gravitational redshift of 28.4 ± 4.8 km s^{-1} is derived from an *IUE* high-dispersion spectrum. Conclusions regarding the mass and radius of CD −38°10980 are also presented.

Subject headings: stars: individual — stars: white dwarfs — ultraviolet: spectra

I. INTRODUCTION

As the number of known white dwarfs has grown, and theoretical understanding of their atmospheres has matured, it is inevitable that observations have concentrated on either demographic and statistical studies or focused on unusual or extreme objects. In this paper we focus on a single DA white dwarf, CD −38°10980 (WD 1620−391, Gr 274), which is unusual only in that it is relatively bright and possesses a well-separated main-sequence companion.

Although one of the brightest known white dwarfs, $V = 11.00$, CD −38°10980 has had a brief observational history, first being classified as a DA white dwarf by Stephenson, Sanduleak, and Hoffleit (1968) from an objective prism spectrum. An interpretive study of this star containing references to earlier work is that of Wegner (1978) who discussed the parallax, photometry, and Balmer profiles in conjunction with determining the gravitational redshift. From photometry and Balmer profiles, Wegner adopted a $T_{\rm eff} = 25{,}500$ K, and estimated log $g = 8.2 \pm 0.25$ with the aid of the measured redshift. A principal uncertainty concerning CD −38°10980 has been its distance, with a discrepancy between the photometric parallax of the primary and the astrometric parallax of the white dwarf (Wegner 1978). As a DA, CD −38°10980 was also included in the large sample of white dwarfs studied by Koester, Schulz, and Weidmann (1979). They determined a somewhat lower temperature and gravity for this object. Most recently a temperature of 24,500 K was determined for CD −38°10980, as a by-product of a detailed analysis of *Voyager 2* observations of the Sirius system (Holberg, Wesemael, and Hubený 1984).

This paper's primary goal is to investigate thoroughly the degree of consistency between a diverse set of observations for a particular DA, CD −38°10980, and model atmosphere calculations. One result of this investigation will be a single model atmosphere, characterized by an effective temperature and surface gravity, which provides an acceptable fit to the observed energy distribution and line profiles. This inquiry has three motivations. First, to what extent can existing DA model atmospheres be relied upon? Second, how well do the various observations, particularly in the ultraviolet, live up to their claimed accuracies? Third, to what degree is it possible to advance the observational status of CD −38°10980?

Of the observations discussed here, only the *IUE* data are completely new. The *Voyager* results have been introduced previously (Holberg, Wesemael, and Hubený 1984) and the bulk of the ground-based data has been discussed in Wegner (1978). In addition none of the analytical techniques employed here are totally unique, although in several instances they constitute significant extensions of previous methods, particularly in the treatment of Lyman-α (Lyα) profiles. What is important in our approach is that all of these techniques are methodically applied to a single star, using a uniform self-consistent grid of model atmospheres.

The various observations of CD −38°10980 are briefly discussed in § II. Section III describes the grid of model atmospheres used to analyze the observations. Following this, each aspect of the data, the *Voyager* observations, *IUE* energy distribution, Lyα profile, Balmer profiles, and photometry is analyzed in turn. In §§ IV and V, we discuss the conclusions which can be drawn from comparisons of model atmospheres and observations. Here we also present a new gravitational redshift deduced from sharp-lined spectral features seen in *IUE* high-dispersion data and discuss the mass and radius of CD −38°10980.

II. OBSERVATIONS

The CD −38°10980 observations analyzed here are diverse and encompass virtually all observable aspects of the spectrum. These observations include photometric, spectrophotometric,

[1] Guest Observer with the *International Ultraviolet Explorer Satellite.*

TABLE 1

OBSERVATIONS OF CD −38°10980

A. *Voyager* OBSERVATIONS

Date	On-Axis/Off-Axis (s)	Reference
1980 Dec 22	4320/7530	Holberg, Wesemael, and Hubený (1984)

B. *IUE* OBSERVATIONS

Image Sequence Number	Dispersion/Aperture	Exposure (s)
SWP 20340	low/large	110.0
SWP 20340	low/small	220.0
SWP 17013	low/large	120.0
LWR 14409	low/large	240.0
SWP 18290	high/large	7200.0

C. GROUND-BASED OBSERVATIONS

Band/Profile	Reference
$V = 11.00$	Wegner 1973*a*
$B-V = -0.145$[a]	Wegner 1973*a*
$U-B = -0.955$	Wegner 1973*a*
$y = 11.00 \pm 0.00$	Wegner 1979
$b-y = -0.097 \pm 0.001$	Wegner 1979
$u-b = +0.005 \pm 0.003$	Wegner 1979
$m_1 = +0.209 \pm 0.001$	Wegner 1979
$c_1 = -0.219 \pm 0.004$[b]	...
Hα	Wegner 1978
Hβ	Wegner 1973*a*
Hγ	Wegner 1978

[a] Incorrect sign for $B-V$ contained in Wegner 1973*a*.
[b] c_1 calculated from $c_1 = (u-b) - 2(b-y) - 2m_1$.

and spectroscopic data ranging from the far-ultraviolet through the visual. Table 1 summarizes the various data and their sources.

a) Voyager Observations

The *Voyager 2* fluxes for CD −38°10980 are the 950–1150 Å fluxes briefly introduced by Holberg, Wesemael, and Hubený (1984) in connection with Sirius B. The *Voyager 2* spectrum shown in Figure 1 exhibits a broad Lyβ feature at 1026 Å as well as continuum crest between Lyβ and Lyα. The spectrum has been truncated at 1150 Å due to increased scattered Lyα sky background. Absolute calibration of the fluxes is discussed in Holberg *et al.* (1982).

b) IUE Energy Distribution

In order to characterize the ultraviolet energy distribution of CD −38°10980 we have constructed a 1250–3200 Å continuum from the *IUE* SWP and LWR data. Two low-resolution, large-aperture SWP images of CD −38°10980 (23040 and 17013) exist. We compared these images, which were separated in time by 8 months, by forming a spectral ratio. This ratio displayed no wavelength correlation and had a mean differing from unity by less than 2%. We therefore averaged both images to improve the signal-to-noise ratio. The SWP and LWR fluxes agree well in the area of overlap and were therefore combined with no adjustment. The resulting spectrum has more resolution than necessary to represent the continuum of CD −38°10980. In order to reduce the amount of computation in subsequent model fitting we have averaged this continuum at 10 Å intervals between 1250 and 1300 Å in the far red wing of Lyα, and at 20 Å intervals between 1300 and 3200 Å. Intervals containing camera artifacts were deleted. The resulting 81 point energy distribution is shown in Figure 2. For a DA white dwarf such as CD −38°10980 the natural expectation is that this wavelength region should contain no features, except for very weak narrow-lined features which have no effect on the ultraviolet energy distribution (Bruhweiler and Kondo 1981, 1982, 1984). In a number of cooler DA white dwarfs, however, there are observations of a broad, shallow feature centered at 1391 Å and of a further trough near 1600 Å. These features have been identified as satellite lines of H I (Nelan and Wegner 1985; Koester *et al.* 1985). Careful examination of all SWP images reveals no evidence for these features in our data, which agrees with Nelan and Wegner who show that the 1400 Å feature disappears at temperatures exceeding 19,000 K.

In the remainder of this paper we will consider two absolute calibrations for the continuum fluxes. One is the "standard" SWP calibration defined by Bohlin and Holm (1980). The other calibration is a modification of the "standard" calibration determined by Hackney, Hackney, and Kondo (1982). This calibration, which we will refer to as the "modified calibration," is defined for SWP wavelengths longer than 1250 Å. Both calibrations yield virtually identical results when the entire energy distribution is considered. The chief advantage of the modified calibration is that it reduces wavelength-

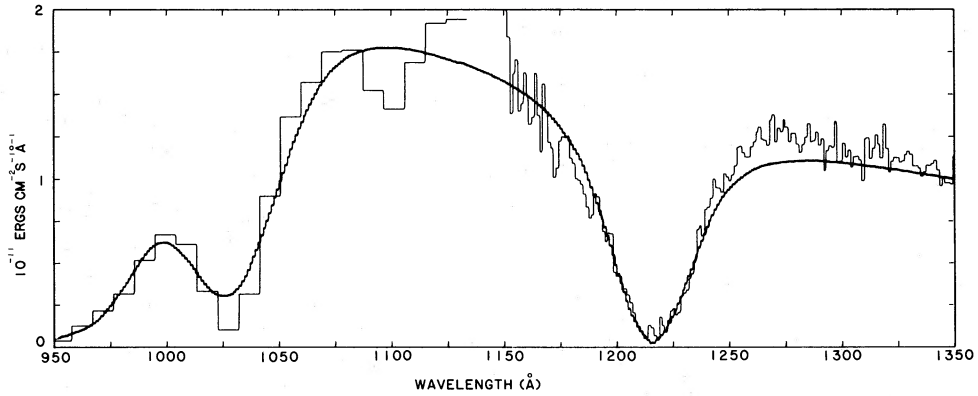

FIG. 1.—The combined *Voyager* and *IUE* fluxes for CD −38°10980 compared with our reference model in the region of the Lyman series. Between 950 and 1150 Å the model fluxes have been convolved with the 25 Å *Voyager* resolution function. In the 1150 and 1250 Å region the *IUE* fluxes were obtained from a small-aperture exposure following normalization to the larger aperture fluxes as described in § IIc.

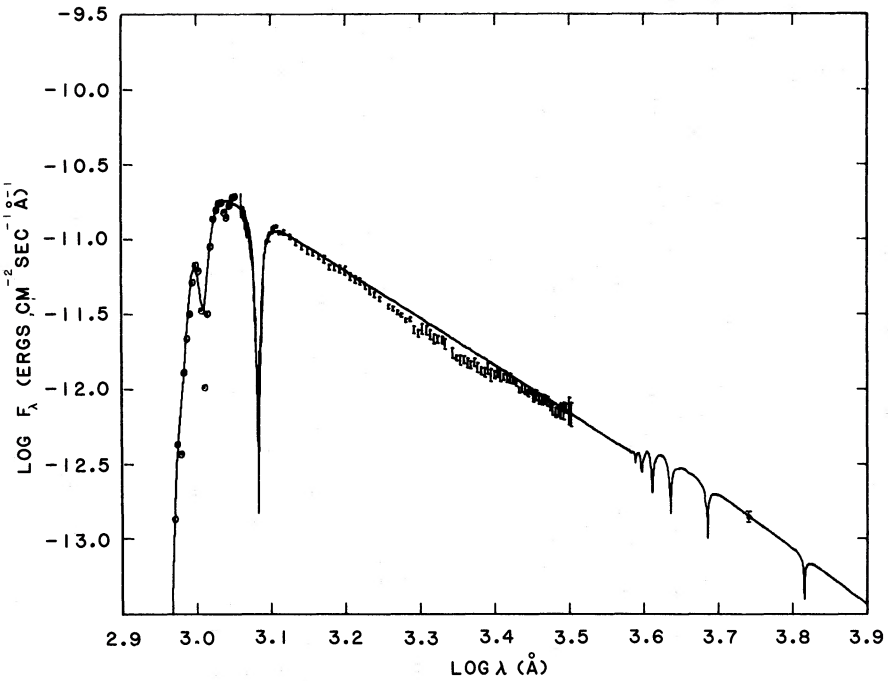

FIG. 2.—The complete energy distribution of CD −38°10980. The reference model (*heavy solid line*) is compared with observed *Voyager 2* (*circles*) and *IUE* fluxes. *IUE* fluxes between log $\lambda = 3.06$ and 3.10 (*light solid line*) are derived from the small-aperture data, while those between 3.10 and 3.51 are derived from large-aperture data and are represented as single error bars at 20 Å intervals. A single flux point derived from the visual magnitude ($V = 11.00$) is shown with accompanying error bar. The decline of the observed flux relative to the model between log $\lambda = 3.25$ and 3.4 is due to the time dependent decline in *IUE* sensitivity described in § III*b*.

dependent undulations in the continuum, as claimed by Hackney, Hackney, and Kondo, and yields smaller postfit residuals.

c) IUE Lyman-Alpha Profile

An adequately exposed *IUE* SWP image can yield useful measurements of flux at wavelengths as short as 1150 Å. In principle, therefore, we could use the averaged large-aperture SWP fluxes discussed in the previous section to define a Lyα profile for CD −38°10980 extending well into the short-wavelength wing. Several factors, however, combine to limit the usefulness of such large-aperture data. First, a superposed geocoronal Lyα emission line can strongly contaminate the core of the Lyα profile. This is especially true for the SWP 20340 large-aperture image. Second, all such spectra contain a reseau near 1190 Å which breaks the continuity of the short-wavelength wing of Lyα. As is well known, substantial improvements in Lyα profiles result if SWP spectra are obtained through the small aperture. The chief advantages are at least a factor of 10 reduction in the geocoronal contamination and an absence of the annoying reseau feature at 1190 Å. The penalties associated with small-aperture images are an increase in exposure time and the loss of absolutely calibrated fluxes. The latter disadvantage is almost entirely overcome if a double exposure of the object is made through the large and small apertures. It is then possible to scale the small aperture fluxes to those of large aperture and obtain a clean Lyα profile on an absolute scale.

Consequently a doubly exposed image of CD −38°10980, SWP 20340, was acquired and used to construct the composite Lyα profile in Figure 1. First, an "effective" SWP exposure time of 127 s was estimated for the extracted small-aperture image from the mean of the spectral ratio of the large- to small-aperture fluxes (avoiding the geocoronal Lyα feature and camera artifacts). This spectral ratio displayed no overall dependence on wavelength. Following this, a composite Lyα profile was formed by joining the small-aperture and large-aperture fluxes at 1250 Å. There are two reasons for choosing large-aperture fluxes to define the continuum level longward of 1250 Å. First, in addition to having higher signal-to-noise ratio, the large-aperture fluxes must be considered more reliable from the standpoint of having been more thoroughly investigated during the establishment of the SWP calibration. Second, we will later find it convenient to use the modified SWP calibration which is defined for large-aperture fluxes longward of 1250 Å.

Rather than averaging the Lyα profile data over an interval comparable to the ~6 Å resolution of a low-resolution SWP image we have retained the ~1.2 Å sampling interval of the extracted SWP fluxes. Uncertainties were assigned to each data point by computing residuals with respect to a smooth cubic spline fit to the Lyα profile. Each point in a 10 Å bin received an uncertainty equal to the root mean square of the residuals within that bin.

d) IUE High-Dispersion Spectrum

A high-dispersion SWP spectral image of CD −38°10980 (Table 1) obtained through the large (10″ × 22″) aperture was acquired from the archival data base of the National Space Science Data Center. These data were analyzed with a technique which utilizes the good internal wavelength scale (±2 km s^{-1}) of the *IUE* to reveal weak sharp-lined spectral features against the essentially flat continuum of the white dwarf. In this technique, all flux data around selected wavelengths corresponding to strong transitions of ions of cosmically abundant

species (usually resonance transitions) are converted to velocity (v) information. Here the velocity is expressed by $v = c(\lambda - \lambda_0)/\lambda_0$, where c is the speed of light, and λ_0 is the laboratory rest wavelength (Kelly and Palumbo 1973), while λ is the wavelength in the unaltered wavelength scale provided by the *IUE Observatory*. Then, the transformed data for the strongest transitions of the same ion, or ions of similar ionization potentials, are co-added to enhance the detection of the searched-for ionic species.

This technique was successful in identifying a set of sharp features at a common velocity in CD −38°10980. These features, which are clearly not interstellar, are presumed to originate with the white dwarf. Features of Si II corresponding to λλ1260.421, 1264.737, and 1265.001 are seen. Of Si III, the resonance transition λ1206.51, and six subordinate transitions of the "metastable-like" ^3P–$^3P^o$ multiplet near 1300 Å are clearly present. The resonance doublet of Si IV near 1400 Å may also be present at or near the detection limit. In Figure 3 we show examples of features due to Si II and Si III. The velocity centroid of the white dwarf features indicate a stellar heliocentric radial velocity of $+38.5 \pm 4.7$ km s^{-1}. This velocity should be contrasted with a velocity of -33.6 ± 4.5 km s^{-1} which is found for another set of features including the O I λ1304 and Si II λ1260 features seen in Figure 3. These features are clearly of interstellar origin, probably originating within the local cloud (Bruhweiler 1982). If we assume that this radial velocity is due to a "uniform flow" resulting from the relative motion of the Sun with respect to the cloud (Crutcher 1982; Bruhweiler and Kondo 1982), then the interstellar velocities seen toward CD −38°10980, if due to this motion may be too negative by approximately 5, but not more than 10 km s^{-1}. Variations and dispersions among various data indicate that this flow may not

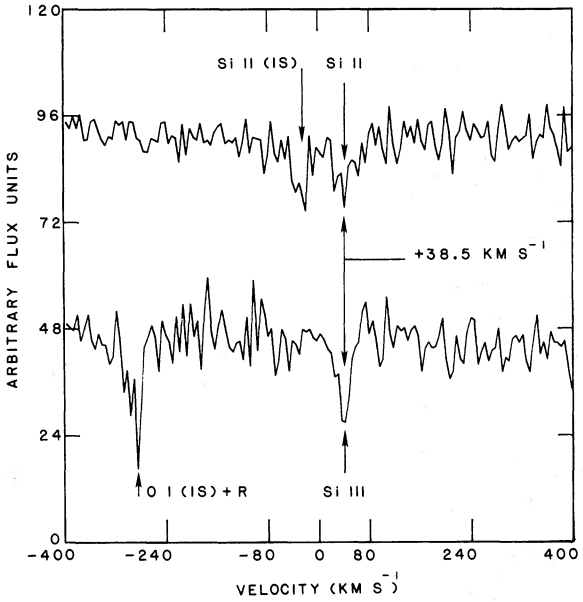

FIG. 3.—Co-added Si II and Si III features seen in CD −38°10980. The upper spectrum is the summed flux data for the Si II transitions λλ1260.421. 1264.737, and 1265.001. The component near −30 km s^{-1} is due to the addition of interstellar Si II λ1260.421 near that velocity with nearby interstellar Si II λλ1264.737 and 1265.001. The lower spectrum is the summed data of the Si III ^3P–$^3P^o$ transitions λλ1294.543, 1298.926, and 1303.320. The features near −300 km s^{-1} are due to contributions of a reseau and interstellar O I near 1302 Å. The white dwarf photospheric velocity component at +38.4 km s^{-1} is clearly visible in the Si II and Si III data.

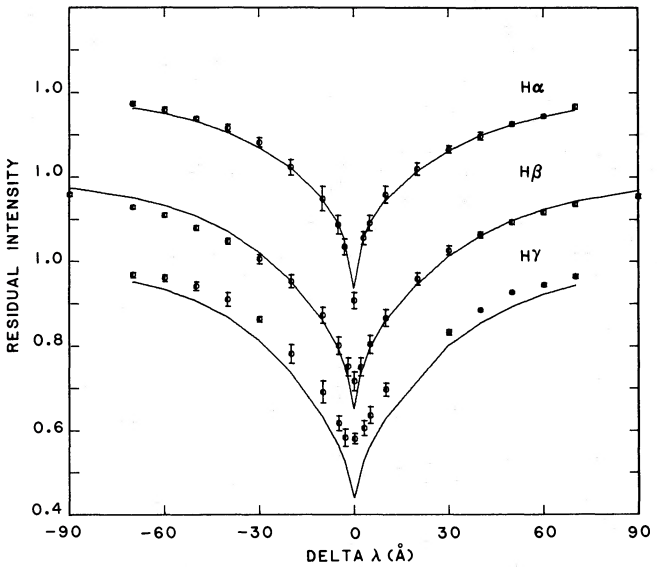

FIG. 4.—A comparison of the Balmer line profiles of CD −38°10980 with those of our reference model. Results are discussed in § IIIe.

be perfectly uniform or that the exact speed and direction of the wind is not well determined, so that detailed agreement should not necessarily be expected. In summary, the interstellar radial velocity toward CD −38°10980 is consistent with the first-order predictions of uniform flow. A more detailed discussion of *IUE* velocity measurements and the sharp-lined features in this star and other white dwarfs can be found elsewhere (Bruhweiler 1984; Bruhweiler and Kondo 1984).

e) *Balmer Profiles*

In determining the gravitational redshift of CD −38°10980, Wegner (1978) used measurements of the Hα, Hβ, and Hγ profiles to help constrain the temperature of CD −38°10980. In that study, model profiles of various temperatures were compared with averages of the red and blue wings of each line. For our investigation we have returned to the original residual intensity measurements in order to obtain bilateral profiles of each line. These profiles, shown in Figure 4, are derived from two independent sources. The Hα profile originates from Radcliffe Observatory coudé plate material described in Wegner (1978), while the Hβ and Hγ profiles originate from Cassegrain image-tube spectra obtained at Mount Stromlo Observatory (Wegner 1973*a*). For the Hα profile, mean residual intensities and associated uncertainties have been computed from the original measurements of the five plates described in Wegner (1978). Similar computations were made from the original Hγ profile measurements of four Mount Stromlo plates. In the case of Hβ, only the profile tabulated in Wegner (1973*a*) was available so that uncertainties were estimated from the corresponding Hγ uncertainties.

III. ANALYSIS

a) *White Dwarf Model Atmospheres*

The model atmospheres employed in our analysis of CD −38°10980 are extensions of Wesemael *et al.* (1980). Briefly, they assume LTE, plane-parallel geometry, and a pure hydrogen composition and include hydrogen line blanketing. An enhancement facilitating analysis of *Voyager* fluxes and the Lyα profile has been the computation of detailed synthetic

spectra of the Lyman series down to and including the 1–7 transition (λ931). These calculations make use of the unified Stark-broadening theory of Vidal, Cooper, and Smith (1973) up to Lyδ, and of the results of Edmonds, Schluter, and Wells (1967) for higher transitions. Emergent fluxes were computed for wavelengths extending to the *IUE* long-wavelength limit at 3200 Å. Up to this point, the models are analogous to those employed in the analysis of Sirius B by Holberg, Wesemael, and Hubený (1984). In order to provide a consistent basis for the analysis of the observed Balmer profiles, each model also includes the emergent fluxes within ± 150 Å of the Hα, Hβ, and Hγ lines. In those segments of the analysis where gravity plays a significant role, such as in the Balmer and Lyman series profiles, models were interpolated from within a grid of $\log g = 7.5$, 8.0, and 8.5 and temperatures of 24,000, 25,000, and 26,000 K. For the continuum energy distribution where gravitational effects are insignificant, a one-dimensional grid of models having $\log g = 8.0$ and temperatures in the range 20,000–30,000 K was employed.

Finally, at this point it is convenient to anticipate a final result and introduce what we will call our "reference model." This model has a temperature of 24,700 K and $\log g = 7.95$ and will be shown to be the single model best capable of describing our various observations of CD $-38°10980$. We will consistently use this model to exhibit comparisons with observation.

b) *Continuum Energy Distribution*

By itself the 1250–3200 Å *IUE* energy distribution lacks a sufficient wavelength base to provide a sensitive indication of effective temperature. Much better estimates can be obtained by extending the wavelength baseline of measured fluxes to significantly longer wavelengths. We have therefore used the observed visual magnitude of CD $-38°10980$ (Table 1) to provide a measure of apparent monochromatic flux at 5500 Å. Conversion to monochromatic flux assumes an absolute flux from Vega of 3.57×10^{-20} ergs cm^{-1} s^{-1} Hz^{-1} near 5500 Å (Tüg, White, and Lockwood 1977). The model fluxes are related to the observed visual and *IUE* fluxes through the fundamental relation

$$f_\nu = 4\pi H_\nu R^2/D^2 , \quad (1)$$

where f_ν is the observed absolute flux and H_ν is the monochromatic Eddington flux in ergs cm^{-2} s^{-1} Hz^{-1} sr^{-1}. The quantity R^2/D^2, involving the stellar radius R and the distance D, represents the stellar solid angle.

In fitting model atmosphere continua to the observed energy distribution, we are seeking to determine the effective temperature $T_{\rm eff}$ and the solid angle by applying two separate constraints to the models. First is the constraint imposed by the visual magnitude. From the 5500 Å model atmosphere fluxes we have derived a simple analytic expression for the Eddington flux in terms of the effective temperature,

$$\log H_\nu = -4.445 + 0.0354 T_3 - 9.816 \times 10^{-5} T_3^2 , \quad (2)$$

where $T_3 = T_{\rm eff}/1000$. This expression is valid over the range $20 < T_3 < 30$ and represents H_ν to better than 1%. We will employ this relation throughout the rest of this section and assign a collective uncertainty of 3.3% to the resulting values of R^2/D^2. This uncertainty (following Shipman 1979) has components of 1% (visual magnitude), 1% (absolute calibration), and 3% (model accuracy). The second constraint is the *IUE* energy distribution. There are numerous ways to apply this constraint. We will employ a least-squares fit to the *IUE* energy distribution.

An overall fit to the *IUE* energy distribution, constrained by the visual magnitude, yields $T_{\rm eff} = 23{,}925 \pm 500$ K. While such a temperature is in reasonable agreement with expectations, the *IUE* energy distribution shows several significant deviations from the model continuum. This can be seen in Figure 2 where we compare our reference model with the combined *IUE* SWP and LWR energy distribution. The most significant deviations from the model can be characterized as a 10%–20% "sag" in the *IUE* fluxes relative to the model between 1750 and 2500 Å. There is no known opacity source, in the almost pure hydrogen atmosphere of CD $-38°10980$, which can account for such lower than expected fluxes. Neither is it possible to remove the "sag" by dereddening the energy distribution. Some understanding of the "sag" is possible if we consider reasonable modifications to the *IUE* sensitivity, in particular wavelength-dependent, secular declines in camera sensitivity. Two different approaches have been taken to this problem. Holm (1984) has monitored the sensitivity of the LWR camera between late 1978 and mid-1983, through comparisons of three standard stars. From this analysis he has determined wavelength-dependent rates of sensitivity decline in the LWR at 25 Å resolution. If we correct our LWR data for this sensitivity decline, we find a considerable improvement in the LWR residuals with respect to our reference model. Similar declines have been documented for the SWP (Sonneborn and Garhart 1983); however, the present data only refer to broad bands of several hundred angstroms in width. A different approach has been taken by Finley, Basri, and Bowyer (1984). Using a large sample of *IUE* observations of DA white dwarfs, grouped into three epochs between 1979 and 1983, they determined wavelength-dependent sensitivity declines for both cameras. Their technique was to employ existing optical data to establish an initial temperature scale and then to produce a model-determined correction vector which yielded internally consistent UV fluxes for a sample of white dwarfs at each epoch. CD $-38°10980$ was among the stars in the Finley, Basri, and Bowyer sample, and their corrected fluxes differed by typically less than 5% from their continuum model at all wavelengths. The revised *IUE* temperature which they derive for CD $-38°10980$ is $24{,}570^{+390}_{-370}$ K, in excellent agreement with our reference model. Since we derive no direct results from the *IUE* continuum fluxes we have chosen not to employ the suggested corrections but simply to display (Fig. 2) the comparison between the observations and our reference model.

c) *Voyager Data*

For a white dwarf in the temperature range of CD $-38°10980$, gravity should have a significant influence upon the continuum fluxes in the 1000 Å region due to the overlap of the Lyγ and Lyβ wings. We have therefore fitted the *Voyager* fluxes shown in Figure 1 with a grid of model atmospheres of varying temperature and gravity. The procedure followed in fitting these models was to assume a fixed solid angle and then to compute a lattice of χ^2 values with models interpolated from our original 3×3 grid. The model corresponding to the best fit to the *Voyager* data is located at $T_{\rm eff} = 24{,}600$ K and $\log g = 8.1$. This model has a χ^2 per degree of freedom, χ^2/ν, of 1.1. The contour representing the 95% confidence interval is shown in Figure 5. As can be seen, temperature and gravity are correlated.

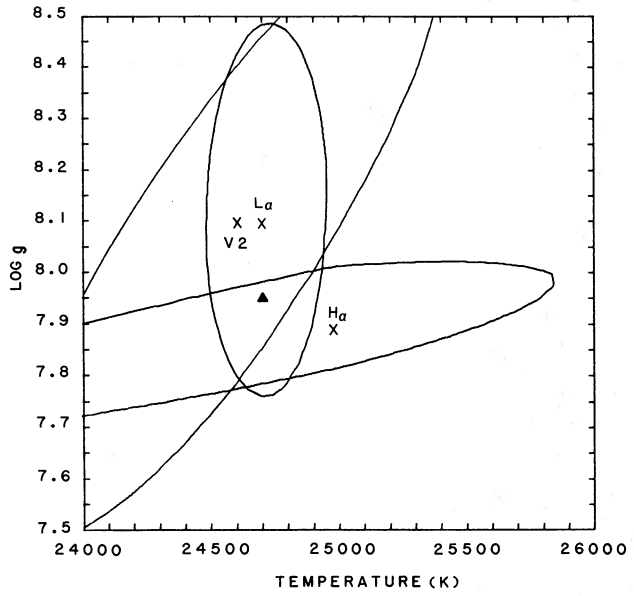

FIG. 5.—Contours of equal χ^2 representing three independent determinations of the effective temperature and surface gravity for CD −38°10980. The narrow, horizontally oriented contour is derived from an analysis of the Hα profile (§ III*e*). The vertically oriented ellipse is derived from an analysis of the Lyα profile (§ III*d*). The broad sloping contour is derived from an analysis of the *Voyager* fluxes (§ III*c*). The temperatures and gravities corresponding to the best fitting models obtained for each of the three analyses are indicated by the X's labeled Hα, Lα, and V2, respectively. The location of our reference model (▲) is also shown. Note the near orthogonality between the Lyα and Hα contours. This illustrates the ability to separate the effects of temperature and gravity through the joint analysis of Lyα and Hα profiles.

d) Lyman-Alpha Profile

We have fitted the Lyα profile shown in Figure 1 with a grid of model atmospheres of varying temperature and gravity. The fitting procedure was identical to that employed for the *Voyager* data. The resulting region of the temperature-gravity plane describing models which minimize χ^2 is shown in Figure 4. In this region the best fitting model has an effective temperature of 24,700 K and a gravity of log $g = 8.1$. For this model the minimum value of χ^2/ν is 2.6. Such a value is large; however, it is calculated on the assumption that the observational uncertainty of the individual data points can be solely represented by the scatter of the data about a smoothed curve. An examination of the actual fit of the model to the data reveals that the model provides a quite adequate representation of the data. This is evident in Figure 1 where we plot our reference model, which differs only slightly from the best fit Lyα model. Judged by the qualitative standards of previous discussions of *IUE* Lyα profiles the fit is more than satisfactory. The only major systematic difference which could significantly bias our results is the apparent excess evident in the long wavelength shoulder of Lyα. This excess is somewhat reduced, but still present, even in the best fitting model. It is tempting to attribute the bulk of this excess to subtle, wavelength-dependent, errors in the *IUE* absolute fluxes, such as those discussed by Hackney, Hackney, and Kondo (1982). It is also conceivable, however, that slight departures from the Vidal, Cooper, and Smith (1973) treatment of broadening in the Lyα wings may exist. Such departures have been discussed on theoretical grounds (Feautrier, Tran Minh, and Van Regemorter 1976; Le Quang Rang and Voslamber 1981). In the future it will be possible, through careful investigation of a wide range of DA white dwarf Lyα profiles at various temperatures, to discriminate between these two possibilities (Holberg and Wesemael 1984). Having at present no independent means of estimating such effects, we will accept as valid the results given by the fit and regard the uncertainty in our results as being 150% of the minimum χ^2. The region of the temperature and gravity plane corresponding to this choice is seen in Figure 5. One significant aspect of the fit to the Lyα profile immediately apparent in Figure 5 is the relatively good temperature discrimination and the near total absence of a correlation with gravity. The latter effect has been noted previously by Greenstein and Oke (1979).

e) Balmer Profiles

Measured Balmer profiles exist for CD −38°10980 (see § II*d*), and we analyze them in a manner similar to our treatment of Lyα. This was done for Hα, Hβ, and Hγ by comparing them with our model grid in the $T_{\rm eff}$–log g plane. Residual intensities were employed rather than absolute fluxes, as for Lyα. Results for the three Balmer profiles are mixed. For Hα it is possible to achieve an excellent fit over a range of $T_{\rm eff}$ and log g consistent with our expectations for CD −38°10980. The best fitting model corresponds to $T_{\rm eff} = 24{,}800$ K and log $g = 7.9$ with a χ^2/ν of 0.63. The Hα profile is relatively insensitive to temperature but a good discriminant of gravity. In Figure 5 we show the $\chi^2/\nu = 1$ contour for the Hα profile. In Figure 4 we compare the reference model Hα profile with the observed. For Hβ the best fitting model occurs at the high-temperature, high-gravity border of our grid at $T_{\rm eff} = 25{,}900$ K and log $g = 8.4$ with a χ^2/ν of 2.2. Examination of the fit for this particular model shows the excess variance is contributed by positive residuals (observed − expected) on the shoulder of the red wing. For the reference model shown in Figure 4 the opposite behavior can be seen in the blue wing. It is not possible to successfully model both wings simultaneously. The basic reason for this is that the observed profile is significantly less symmetrical than the model profiles. The results obtained for the Hγ profile are even less satisfactory. No minimum χ^2 model existed within our grid. In Figure 4 where our reference model is compared with the Hγ profile the problem is clearly seen to be one of continuum level.

The failure to fit properly the Hγ and, to a lesser extent, the Hβ profiles is discouraging but perhaps not unexpected. We have applied rather stringent statistical standards in our analysis in addition to considering both wings of the Balmer profiles. For example, if only one wing of the Hβ profile is considered or if the profile is made symmetrical by averaging both wings, a fit which appears reasonable can be obtained. Such results, however, retain a large χ^2 and an affinity for the edge of our grid. In the case of the Hγ profile if we allow arbitrary adjustments to the continuum level considerable improvement is also possible. In both cases the fits obtained appear qualitatively acceptable, but this does not necessarily lend confidence to the results. Indeed, our experience in fitting Balmer line profiles in DA white dwarfs indicates that fits comparable to our Hα results can be obtained for other DA's. The difficulties encountered in fitting our Hβ and Hγ profiles emphasize the need to obtain such measurements with modern linear detectors and to have good knowledge of both the continuum level and the relative detector response across the entire line profile. It is probably premature to conclude that either observation or broadening theory is at fault, without the reobservation of both lines. We instead consider only the Hα

profile, which was obtained independently of the Hβ and Hγ profiles.

We have used the Hα profile primarily as a gravity indicator. This may appear somewhat surprising, as the lowest Balmer lines are frequently employed as temperature indicators while overlapping higher Balmer lines (Hδ, Hε, etc.) are usually considered better surface gravity determinants (Schulz and Wegner 1983). When Hα is used to determine temperature, it is tacitly assumed that gravity is a fixed quantity (usually taken to be log $g = 8$). If, as some studies (Koester, Schulz, and Weidemann 1979) have shown, most DA white dwarfs lie within a narrow range of masses, then a well-defined mass-radius relationship will yield a correspondingly narrow range of gravities. Under such circumstances the relative importance of temperature in determining Balmer profiles is enhanced, and unique temperatures can be obtained. However, in many cases the uncertainty regarding surface gravity ultimately limits the accuracy of temperatures determined from Balmer profiles. For example, an uncertainty of ± 0.15 in log g for CD $-38°10980$ (this is approximately the same size as the range of gravities resulting from the $\pm 0.1\ M_\odot$ range of DA masses discussed by Koester, Schulz, and Weidmann 1979) corresponds to a ± 1350 K uncertainty in temperature in our analysis of the Hα profile. The point is that, in the temperature range we are considering, the overall energy distribution, the Lyα profiles or visual colors all provide more accurate estimates of temperature than a single-parameter determination of temperature based on Balmer profiles alone. Thus, in our case, the sensitivity of the Hα to atmospheric parameters is put to best use by taking advantage of the residual gravity sensitivity of that line to constrain log g.

f) Photometry

Our results concerning CD $-38°10980$ can be related to two recent studies (Shipman 1979; Koester, Schulz, and Weidemann 1979) which have systematically applied photometry to the determination of atmospheric parameters for large samples of white dwarfs. In the case of Koester, Schulz, and Weidemann, comparison is immediate as CD $-38°10980$ was included in their sample of white dwarfs. Their optimum solution, utilizing the Wegner (1979) *ubvy* photometry, was $T_{\rm eff} = 24{,}532 \pm 653$ K and log $g = 7.39 \pm 0.36$. Shipman did not include CD $-38°10980$ in his sample. However, Holberg, Wesemael, and Hubený (1984) have transformed the Wegner *ubvy* photometry into the bands employed by Shipman and obtained $T_{\rm eff} = 24{,}250^{+750}_{-1000}$ K with no estimate of the gravity. Thus, existing methods and photometry yield reassuringly consistent estimates of the temperature for CD $-38°10980$. However, the gravity obtained by Koester, Schulz, and Weidemann does not lie in a range compatible with any of our results, but at the temperatures under consideration, photometry alone provides essentially no surface gravity information.

IV. DISCUSSION

The constraints on temperature and gravity provided by our analysis of the Lyα profile, the Balmer-α profile, and the *Voyager* fluxes constitute a basis for defining a narrow range of acceptable values for both parameters. Although it is possible to formally determine a single best fit result by devising a weighting scheme involving these three separate constraints, it is just as valid, in light of the possible influences of systematic biases in all three results, to simply estimate our final result from Figure 5. Relying primarily on the tightly constrained temperature provided by the Lyα profile, we estimate $T_{\rm eff}$ to be $24{,}700 \pm 250$ K. The final estimate for gravity is taken to be log $g = 7.95 \pm 0.15$ which represents a compromise between the lower values demanded by the Balmer-α profile and the somewhat higher results preferred by the Lyα profile and *Voyager* results. Our estimated uncertainties for each quantity encompass the three separate best fit values. The solid angle is the only remaining parameter necessary to completely define our reference model on an absolute scale. The value appropriate to our reference temperature and gravity and the observed visual magnitude is $R^2/D^2 = 4.82 \pm 0.18 \times 10^{-22}$.

Before we discuss our new redshift determination, a brief review of existing parallax and gravitational redshift measurements for CD $-38°10980$ is in order. As previously mentioned, Wegner (1978) in reviewing previous parallax determinations found an apparent discrepancy between a best estimate of $0''.058 \pm 0''.009$ based on astrometric measurements and a value of $0''.983 \pm 0''.010$ derived from photometry of the proper motion companion HD 6094. In addition to these values we have recently become aware of a new astrometric parallax for CD $-38°10980$ of $0''.067 \pm 0.004$ (Ianna 1983). The photometric parallax and the Ianna astrometric parallax are marginally exclusive of one another. Since there is no compelling reason to prefer one result over the other and since they represent acceptable extremes for the distance to CD $-38°10980$ we will retain both results and separately consider the consequences of each. Using our solid angle for CD $-38°10980$ these two distance determinations yield stellar radii of $1.45 \pm 0.09 \times 10^{-2}\ R/R_\odot$ (parallax radius) and $1.17^{+0.16}_{-0.13} \times 10^{-2}\ R/R_\odot$ (photometric radius), respectively.

There exist two published gravitational redshift determinations for CD $-38°10980$. This star was included among the binary pairs discussed in Wegner (1973*b*) where a value of $+33 \pm 17$ km s^{-1} was quoted. Subsequently, Wegner (1978) using the same instrumentation to measure radial velocities for both CD $-38°10980$ and HR 6094 made a differential determination of the gravitational redshift of $+44 \pm 7$ km s^{-1}.

In § II*d* we determined that a set of sharp Si II and Si III features seen in the *IUE* high-dispersion image implied an apparent heliocentric velocity of $+38.5 \pm 4.7$ km s^{-1} for CD $-38°10980$. Its G5 V companion HR 6094 has a measured radial velocity of $+10.1 \pm 0.7$ km s^{-1} (Campbell and Moore 1928). Differencing these two results gives a residual $+28.4 \pm 4.8$ km s^{-1} which we associate with the gravitational redshift of CD $-38°10980$. There are two important caveats to this interpretation. First is the unknown systematic difference which may exist between the absolute radial velocity measurements of HR 6094 and CD $-38°10980$. Second is the possibility that the sharp Si II and Si III features may not arise in the photosphere of CD $-38°10980$, but at some distance from the surface, perhaps even in a wind (Bruhweiler and Kondo 1983). In this case our redshift measurement would only represent a lower limit to the actual gravitational redshift. Keeping the above qualifications in mind, we will follow Sion and Guinan (1983) and interpret our result as a true gravitational redshift and examine the resulting consequences.

In Figure 6 we compare the mass and radius constraints implied by our surface gravity and radius determinations with the zero-temperature mass radius relationships of Hamada and Salpeter (1961) for white dwarfs with He, C, and Mg cores. As can be seen, the astrometric and photometric parallaxes define regions of the mass-radius plane which effectively straddle the

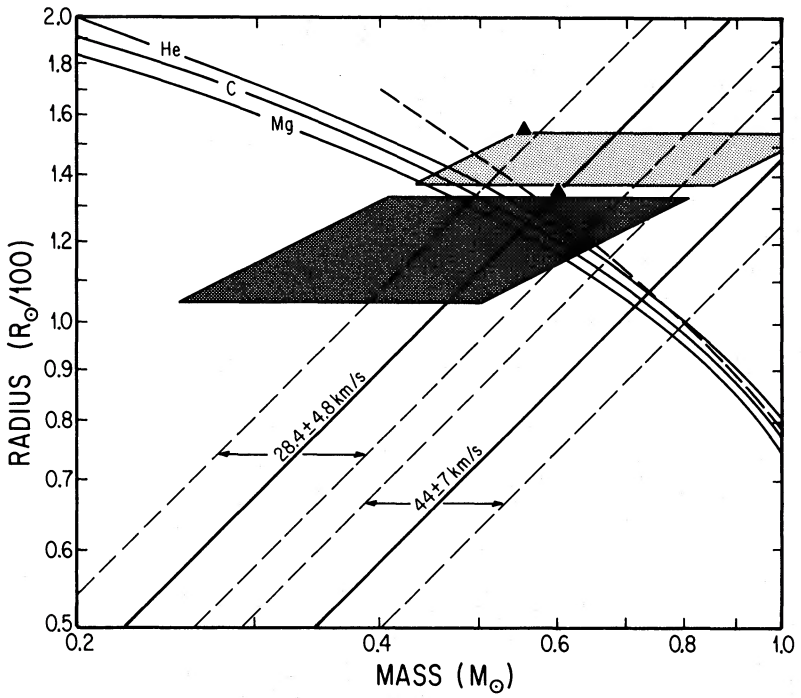

FIG. 6.—A summary of existing constraints on the mass and radius of CD −38°10980. The two shaded parallelograms are derived from our surface gravity determination (log $g = 7.95 \pm 0.15$) together with the two alternate distance estimates for CD −38°10980 discussed in § V. The upper parallelogram corresponds to the latest astrometric parallax (0".067 ± 0".004) while the lower represents the 0".083 ± 0".011 photometric parallax of HR 6094 (Wegner 1978). The two diagonal sets of parallel lines represent the constraints imposed by the gravitational redshift measurement of Wegner (1978) ($+44 \pm 7$ km s^{-1}) and that derived from the *IUE* high-dispersion spectrum ($+28.4 \pm 4.8$ km s^{-1}). Also shown are several different mass-radius relations. The solid curves are zero-temperature, Hamada-Salpeter models for white dwarfs having He, C and Mg cores. The dashed curve represents a cooling sequence for a ^{12}C core with H envelope (Winget, Lamb, and Van Horn 1985), while the solid triangles represent two Koester and Schonberner (1985) models incorporating residual H burning in the stellar envelope.

Hamada-Salpeter mass-radius relations. Zero-temperature models, like those of Hamada and Salpeter, assume complete core degeneracy. There is a question of the extent to which mass-radius relations can be considered truly independent of surface temperature. Two distinct sets of sequences of stellar models can be used to investigate this point. The Winget, Lamb, and Van Horn (1985) cooling sequences consist either of pure ^{12}C cores (see also Lamb and Van Horn 1975) or of carbon cores with thin helium or helium and hydrogen layers. The largest increase over the zero-temperature radii is seen in the latter models: typically, that increase is 6%–15%. The Koester and Schonberner (1985) models incorporate residual hydrogen burning in the stellar envelope (see also Iben and Tutukov 1984). The Koester and Schonberner models predict significantly larger radii for a given temperature and mass. In Figure 6 we show results for two such models having surface temperatures of 25,000 K, hydrogen envelopes of 8×10^{-5} $M_\odot$, and core masses of 0.553 and 0.598 $M_\odot$. These effects produce larger radii as favored by the astrometric parallax. Also shown in Figure 6 are the mass-radius constraints corresponding to the Wegner (1978) gravitational redshift and our new *IUE* result.

Finally, we can directly determine the total luminosity of CD −38°10980. As seen in Figure 2 our reference model provides a very good representation of the observed energy distribution. This being the case, the total luminosity of CD −38°10980 is, by definition, simply $4\pi R^2 \sigma T^4$. Determining the luminosity in this manner is equivalent to a direct integration of the observed *Voyager* and *IUE* fluxes followed by a small (11%) "bolometric-like" correction to account for the flux longward of 3200 Å. (This is the reverse of the normal situation where a large bolometric correction is required to account for the unobserved bulk of the flux in the ultraviolet.) Using our reference temperature and the two distance estimates we arrive at luminosities of $7.06 \pm 1.00 \times 10^{-2}$ and $4.59 \pm 1.1 \times 10^{-2}$ $L_\odot$ for the astrometric and photometric parallaxes, respectively. Both these results lead to a standard bolometric correction of 2.51 ± 0.14 which should be compared with 2.22 for a 24,700 K model from Wesemael *et al.* (1980).

V. CONCLUSION

The principal objective of this investigation has been a detailed examination of the degree of correspondence between model atmosphere calculations for hot DA stars and observations. The results, by and large, are both reassuring and encouraging. The overall energy distribution and the Lyα and Hα profiles are seen to be in good agreement with a single, self-consistent model atmosphere. This model is completely defined by an effective temperature of 24,700 ± 250 K and a surface gravity of log $g = 7.95 \pm 0.15$ and by its assumed pure hydrogen composition. With the possible exception of the long-wavelength wing of Lyα, the discrepancies are relatively minor and likely arise from observational difficulties.

We therefore conclude that existing model atmospheres are reliable tools for the precise determination of DA atmospheric parameters. In particular, we have demonstrated the value of using Lyα profiles to determine temperature and Balmer α profiles to determine gravity. Jointly analyzing Lyα and Balmer profiles with a uniform grid of model atmospheres is shown to provide an effective means of decoupling the effects of temperature and gravity.

We find both *Voyager* and *IUE* fluxes are well represented

by our reference model over the range 950 to 3200 Å. In the case of the *Voyager* fluxes, this can be regarded as evidence that the adopted *Voyager* absolute calibration shortward of 1200 Å (Holberg *et al.* 1982) is in good agreement with predicted fluxes from what is perhaps the simplest example of a stellar atmosphere: a pure hydrogen atmosphere having a well-determined temperature and gravity. In the case of the *IUE* fluxes, a significant discrepancy between model and observation is found over a limited wavelength range. However, this discrepancy is most easily explained by a decline in *IUE* sensitivity.

The improvements in the temperature, gravity, and solid angle arrived at here, together with the new redshift determination and parallax information, provide the basis for a rediscussion of the mass and radius of CD −38°10980. The allowable ranges of mass and radius are marginally consistent with the zero-temperature mass radius relations. However, it is also evident from Figure 6 that a considerable degree of uncertainty remains regarding the mass and radius of CD −38°10980. Some headway can be made by adopting the point of view that, regardless of whether the star is completely degenerate or not, the zero-temperature mass-radius relationships define the minimum possible radius for a given mass and chemical composition. Using the lowest redshift (+23.6 km s^{-1}) consistent with our *IUE* high-dispersion spectrum, we then find a minimum mass of 0.49 $M_\odot$. In the same fashion, the lowest surface gravity consistent with our Hα results (log $g = 7.80$; the right-hand side of the shaded regions) yields a lower limit of 1.18×10^{-2} $R_\odot$ for the radius of CD −38°10980. The upper limit to the radius, given directly by the astrometric parallax, is 1.55×10^{-2} $R_\odot$. A corresponding upper mass limit is not well determined since both the gravity and redshift constraints allow values as large as 0.8 or 0.9 $M_\odot$. Further progress must await a resolution of the differing parallaxes and redshifts. In both instances considerable improvement is certainly possible. The distance to CD −38°10980 is well within the range where better parallax agreement is to be expected, and further redshift determinations would almost certainly lead to a reduction in the remaining uncertainty in this area. That such efforts are worthwhile is evident from Figure 6. For example, if the stellar radius is found to be as large as indicated by the astrometric parallax, then a useful measurement of departure from the zero-temperature mass-radius relations is possible. Similarly, if subsequent ground-based measurements of the gravitational redshift confirm the Wegner (1978) result, it can be reasonably concluded that our *IUE* results refer to a region at least one-half a stellar radius above the photosphere, or possibly a wind. This would in turn be of help in interpreting similar features seen in other hot white dwarfs.

The authors wish to thank Philip Ianna for providing parallax measurements of CD −38°10980 prior to publication and W. T. Forrester for his valuable assistance in the analysis of these data. *IUE* archive material provided by the National Space Data Center, NSDC/WDC-A, is gratefully acknowledged. This work was supported by NASA grants. NAG5-411 and NAGW 587, and by the NSERC Canada.

REFERENCES

Bohlin, R. C., and Holm, A. 1980, *IUE Newsletter*, No. 10, p. 37.
Bruhweiler, F. C. 1982, in *Advances in Ultraviolet Astronomy: Four Years of IUE Research*, ed. Y. Kondo, J. M. Mead, and R. D. Chapman (NASA CP-2238), p. 125.
———. 1984, in *Future of Ultraviolet Astronomy Based on Six Years of IUE Research*, ed. J. M. Mead, Y. Kondo, and R. Chapman (NASA CP-2349), p. 269.
Bruhweiler, F. C., and Kondo, Y. 1981, *Ap. J. (Letters)*, **248**, L123.
———. 1982, *Ap. J.*, **259**, 232.
———. 1983, *Ap. J.*, **269**, 657.
———. 1984, in preparation.
Campbell, W. W., and Moore, J. H. 1928, *Pub. Lick Obs.*, **16**, 239.
Crutcher, R. M. 1982, *Ap. J.*, **254**, 82.
Edmonds, F. N., Jr., Schluter, H. and Wells, D. C., III. 1967, *Mem. R.A.S.*, **71**, 271.
Feautrier, N., Tran Minh, N., and Van Regemorter, H. 1976, *J. Phys. B*, **9**, 1871.
Finley, D. S., Basri, G., and Bowyer, S. 1984, in *Future of Ultraviolet Astronomy Based on Six Years of IUE Research*, ed. Y. Kondo, R. D. Chapman, and J. M. Mead (NASA CP-2349), p. 249.
Greenstein, J. L., and Oke, J. B. 1979, *Ap. J. (Letters)*, **263**, L63.
Hackney, R. L., Hackney, K. R. H., and Kondo, Y. 1982, in *Advances in Ultraviolet Astronomy: Four Years of IUE Research*, ed. Y. Kondo, J. M. Mead, and R. D. Chapman (NASA CP-2238), p. 335.
Hamada, T., and Salpeter, E. E. 1961, *Ap. J.*, **134**, 683.
Holberg, J. B., Forrester, W. T., Shemansky, D. E., and Barry, D. C. 1982, *Ap. J.*, **257**, 656.
Holberg, J. B., and Wesemael, F. 1984, in the *Future of Ultraviolet Astronomy Based on Six Years of IUE Research*, ed. J. Mead, R. D. Chapman, and V. Kondo (NASA CP-2349), p. 285.
Holberg, J. B., Wesemael, F., and Hubený, I. 1984, *Ap. J.*, **280**, 679.
Holm, A. V. 1984, private communication.
Ianna, P. A. 1983, private communication.
Iben, I., Jr., and Tutukov, A. V. 1984, *Ap. J.*, **282**, 615.
Kelly, R. L., and Palumbo, L. J. 1973, *Atomic and Ionic Emission Lines Below 2000* Å (NRL Rept. 7599).
Koester, D., and Schonberner, D. 1985, in preparation.
Koester, D., Schulz, H., and Weidemann, V. 1979, *Astr. Ap.*, **76**, 262.
Koester, D., Weidemann, V., Zeidler, E.-M. K. T., and Vauclair, G. 1985, *Astr. Ap.*, in press.
Lamb, D. Q., and Van Horn, H. M. 1975, *Ap. J.*, **200**, 306.
Le Quang Rang, and Voslamber, D. 1981, *J. Quant. Spectrosc. Rad. Transf.*, **25**, 35.
Nelan, E. P., and Wegner, G. 1985, *Ap. J. (Letters)*, **289**, L31.
Schulz, H., and Wegner, G. 1981, *Astr. Ap.*, **94**, 272.
Shipman, H. L. 1979, *Ap. J.*, **228**, 240.
Sion, E. M., and Guinan, E. F. 1983, *Ap. J. (Letters)*, **265**, L87.
Sonneborn, G., and Garhart, M. P. 1983, *IUE Newsletter* No. 23, p. 23.
Stephenson, C. B., Sanduleak, N., and Hoffleit, D. 1968, *Pub. A.S.P.*, **80**, 92.
Tüg, H., White, N. M., and Lockwood, G. W. 1977, *Astr. Ap.*, **61**, 679.
Vidal, C. R., Cooper, J., and Smith, E. W. 1973, *Ap. J., Suppl.*, **25**, 37.
Wegner, G. 1973*a*, *M.N.R.A.S.*, **163**, 381.
———. 1973*b*, *M.N.R.A.S.*, **165**, 271.
———. 1978, *M.N.R.A.S.*, **182**, 111.
———. 1979, *A.J.*, **84**, 9.
Wesemael, F., Auer, L. H., Van Horn, H. M., and Savedoff, M. P. 1980, *Ap. J. Suppl.*, **43**, 159.
Winget, D. E., Lamb, D. Q., and Van Horn, H. M. 1985, in preparation.

F. C. BRUHWEILER: Department of Physics, Catholic University of America, Washington, DC 20064

J. B. HOLBERG: Lunar and Planetary Laboratory, University of Arizona, 3625 East Ajo Way, Tucson, AZ 85713

G. WEGNER: Department of Physics and Astronomy, Dartmouth College, Hanover, NH 03755

F. WESEMAEL: Département de Physique, Université de Montréal, C.P. 6128, Montréal, Québec H3C 3J7, Canada